

Collisional broadening of some $2^1\Delta_g \leftarrow B^1\Pi_u$ lines in Na_2 molecules by optical-optical double resonance spectroscopy

Jing Liu (刘 静)^{1,2}, Kang Dai (戴 康)², and Yifan Shen (沈异凡)²

¹School of Science, Xi'an Jiaotong University, Xi'an 710049

²Department of Physics, Xinjiang University, Urumqi 830046

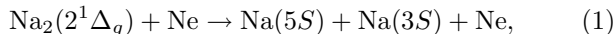
Received January 16, 2006

Using the optical-optical double resonance (OODR) technique, we have studied the collisional broadening of some $2^1\Delta_g \leftarrow B^1\Pi_u$ lines in Na_2 molecules. A single line Ar^+ laser is used to pump the sodium dimers from thermally populated ground state $X^1\Sigma_g^+$ level to the intermediate $B^1\Pi_u$ state. Then, a single-mode diode laser is used to probe the doubly excited $2^1\Delta_g$ state. The broadening rate coefficient is determined from the slope of the total linewidth versus Ne density curve. We obtain the average value $k_{br} = (1.1 \pm 0.5) \times 10^{-8} \text{ cm}^3\text{s}^{-1}$. The collisional excitation transfer between rotational levels of the $B^1\Pi_u$ state (i.e., $B^1\Pi_u(2, 83/84) \leftarrow B^1\Pi_u(2, 82)$) is also investigated. The rates can be determined from the relative intensities of the main peak and satellite lines, combined with a rate equation model. The rates of 1.25×10^6 and $1.07 \times 10^6 \text{ s}^{-1}$ are obtained, respectively.

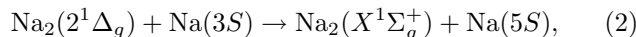
OCIS codes: 020.0020, 020.2070, 020.3690.

In the past few years, photodissociation and collisional excitation transfer of alkali diatomic molecules have been extensively studied^[1–6]. However, most previous spectroscopic studies have involved low-lying states correlating to the ground state and first excited state in the separated atom limit. The range of energies between the low-lying state and the Rydberg state has not been systematically investigated.

In this paper, we have used the optical-optical double resonance (OODR) technique to study the collisional broadening of some $2^1\Delta_g \leftarrow B^1\Pi_u$ lines of Na_2 molecules. In OODR, the first laser (pump) is used to populate one rovibrational level of an intermediate electronic state. The second laser (probe) is then used to excite these molecules to a higher electronic state. In our work, we have excited the ground state $X^1\Sigma_g^+$ to the high-lying state $2^1\Delta_g$ of Na_2 molecules by using the OODR technique. In the present case, collisional line broadening is dominated by collisions with Ne atoms, with a minor contribution from Na atom collisions. Specifically, dissociative collisions such as



quenching collisions such as



as well as elastic line broadening collisions contribute to the overall collision induced broadening linewidth. The collisional broadening rate coefficient is determined from the measured Doppler-free linewidth. The collisional excitation transfer between rotational levels of the $B^1\Pi_u(v', J')$ state is also investigated, and the collisional transfer rate for



is measured, where M represents the perturber which can be any of the species presented in the vapors (Ne,

Na, Na_2).

The experimental setup is shown in Fig. 1. The sodium is contained in a cylindrical Pyrex cell with inner length of 15.0 cm and inner diameter of 2.5 cm using neon as a buffer gas. The cell is sealed after baking and evacuating to 10^{-4} Pa. The cell is placed inside an oven (not shown in Fig. 1), which is heated with a thermistor. The temperature is measured with several thermocouples located at various points on the cell. The temperature of the cell is less than 360°C . The cell is connected by a narrow-bore tube and a greaseless stopcock to a vacuum and gas filling system from which neon gas is admitted as required. Neon pressures of 100–500 Pa are measured with a vacuum gauge. The density of sodium atoms in the vapor phase is obtained by measuring both the wing absorption coefficient and the ratio of the fluorescence to Rayleigh signal^[7].

Two lasers are used to study the two-step excitation of Na_2 molecules. An all line visible Ar^+ laser (Shanghai, Aiao Laser Machinery Co. Ltd, using a prism to select one of the lines) is used to pump sodium dimers in

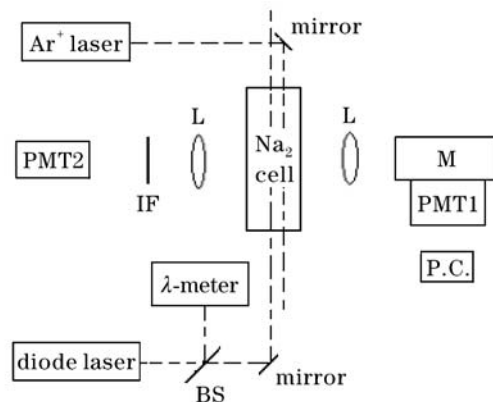


Fig. 1. Experimental setup. IF: interference filter; L: lens; M: monochromator; P.C.: photon counter; BS: beam-splitter; PMT: photomultiplier tube.

the thermally populated ground state levels to the intermediate $B^1\Pi_u$ state. A single-mode diode laser (Tuioptics, frequency range of 820–836 nm, power of 40 mW, linewidth of 5 MHz) is used to excite Na_2 molecules from the $B^1\Pi_u$ state to the $2^1\Delta_g$ state. In this experiment, the Ar^+ laser at 514.5 nm (120 mW, focusing the laser output into the portion of the sample cell produced a power density of about 3 W/cm^2) used as a pump laser to pump a specific level (2,82) of the $\text{Na}_2 B^1\Pi_u$ state from a level (6,83) of the $X^1\Sigma_g^+$ ground state^[8], and the diode laser (the power density of about 1 W/cm^2) populates the $2^1\Delta_g$ level as $2^1\Delta_g(v, 83) \leftarrow B^1\Pi_u(2, 82)$. The two laser beams counterpropagate through the cell. The $2^1\Delta_g \rightarrow B^1\Pi_u$ fluorescence in the direction perpendicular to the laser beams is focused on the slits of 0.66-m monochromator (AM566, Acton), and monitored by a photomultiplier tube (PMT1). A photon counter (M1109, Princeton) records the PMT signals. The total emissions consist of allowed transitions from the $2^1\Delta_g(v, 83)$ level pumped through the two-step process to all possible $B^1\Pi_u(v', 82/83/84)$. To record the OODR spectra, the violet fluorescence emitted from the excited triplet states, mainly $2^3\Pi_g$ and $3^3\Pi_g$, which are populated via collisions from $2^1\Delta_g$, to the $a^3\Sigma_u^+$ state is detected by a filtered photomultiplier tube (PMT2).

In the impact limit, which is appropriate for the conditions of the present experiment, the $\text{Na}_2[2^1\Delta_g(v, J) \leftarrow B^1\Pi_u(v', J') \leftarrow X^1\Sigma_g^+(v'', J'')]$ two-step Doppler-free absorption line shape is a Lorentzian function with full-width at half-maximum (FWHM) Γ , given by

$$\Gamma = \Gamma_p + \Gamma_n + k_{\text{br}}^{\text{Ne}} n_{\text{Ne}} + k_{\text{br}}^{\text{Na}} n_{\text{Na}}, \quad (4)$$

where, Γ_p is the predissociation linewidth, Γ_n is the natural linewidth of the transition, and k_{br}^i represents the broadening rate coefficient, for a particular perturber species with number density n_i .

In this experiment, the density of the neon is $10^{16} - 10^{17} \text{ cm}^{-3}$, while the density of atomic sodium is about three orders of magnitude smaller, so the broadening effect of sodium atoms can be neglected. Equation (4) can be reduced to

$$\Gamma = \Gamma_p + \Gamma_n + k_{\text{br}}^{\text{Ne}} n_{\text{Ne}}. \quad (5)$$

For the $2^1\Delta_g(v, 83) \leftarrow B^1\Pi_u(2, 82)$ transition, we obtain the neon broadening rate coefficient $k_{\text{br}}^{\text{Ne}}$ from the dependence of the measured total linewidth Γ on the neon gas density at fixed temperature (fixed Na atom density). The line widths are measured by scanning the narrow-band $2^1\Delta_g(v, 83) \leftarrow B^1\Pi_u(2, 82)$ transition, while recording the molecular emission. The fluorescence line shape ($2^1\Delta_g(1, 83) \rightarrow B^1\Pi_u(v', J')$) with $n_{\text{Ne}} = 5.0 \times 10^{16} \text{ cm}^{-3}$ is shown in Fig. 2. The total linewidth Γ is measured with an accuracy of about 30 MHz. Figure 3 shows the variation of linewidth with neon atomic density. Combined with Eq. (5), the measured total linewidth versus neon atomic density is well represented by a least squares fitted straight line, whose intercept and slope give $\frac{1}{\tau} = \Gamma_p + \Gamma_n = (2.5 \pm 1.1) \times 10^9 \text{ s}^{-1}$ (τ is the $2^1\Delta_g(v, J)$ state lifetime) and broadening rate coefficient $k_{\text{br}}^{\text{Ne}} = (1.1 \pm 0.5) \times 10^{-8} \text{ cm}^3 \text{ s}^{-1}$, respectively. k_{br} only weakly depends on temperatures (i.e., $k_{\text{br}} \propto T^{0.3[9]}$).

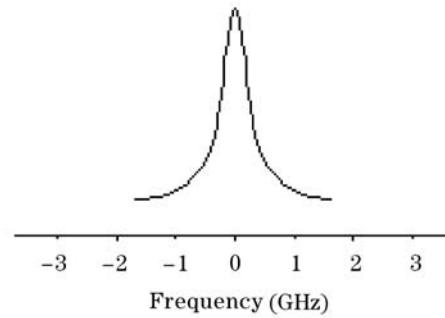


Fig. 2. Probe laser scans over $\text{Na}_2 2^1\Delta_g(1, 83) \leftarrow B^1\Pi_u(2, 82)$ transition. Molecular $\text{Na}_2 (2^1\Delta_g(1, 83) \rightarrow B^1\Pi_u(v', J'))$ fluorescence signal is monitored.

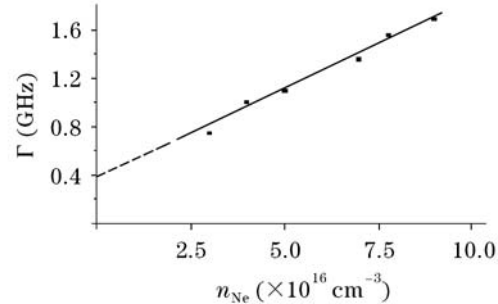
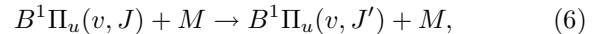


Fig. 3. Plot of the measured linewidth versus neon density for $2^1\Delta_g(1, 83) \leftarrow B^1\Pi_u(2, 82)$ transition.

Moreover, the sources of error in $k_{\text{br}}^{\text{Ne}}$ also involve the broadening effect of sodium atoms. We analogously obtain $k_{\text{br}}^{\text{Ne}} = (1.2 \pm 0.5)$, and $(1.0 \pm 0.5) \times 10^{-8} \text{ cm}^3 \text{ s}^{-1}$ for the $2^1\Delta_g(2, 83) \leftarrow B^1\Pi_u(2, 82)$ and $2^1\Delta_g(3, 83) \leftarrow B^1\Pi_u(2, 82)$ transitions, respectively.

After the $B^1\Pi_u$ state has been prepared by pumping with a separate laser on a particular transition from the ground $X^1\Sigma_g^+$ state, we have observed collisional excitation transfer between different rotational levels of the $B^1\Pi_u$ state



where M represents the perturber which can be any of the species presented in the vapors (Ne, Na, Na_2). The steady-state rate equation for the process of Eq. (6) is of the following form

$$R_{J \rightarrow J'} n_J = n_{J'} / \tau_{J'}, \quad (7)$$

where $R_{J \rightarrow J'}$ is the rate of population transfer from the J to J' level, and $\tau_{J'}$ is the lifetime of the J' level, n_J and $n_{J'}$ are the molecular densities of the $B^1\Pi_u(v, J)$ and $B^1\Pi_u(v, J')$ levels respectively. Equation (7) yields the ratio of the populations in the J and J' levels, $n_{J'} / n_J = R_{J \rightarrow J'} \tau_{J'}$. This ratio is approximately proportional to the fluorescence intensity ratio. Figure 4 shows the main line corresponding to the $2^1\Delta_g(1, 83) \leftarrow B^1\Pi_u(2, 82)$ transition, and the satellite peaks labeled $\Delta J = +1$ and $\Delta J = +2$ are identified as the $2^1\Delta_g(1, 84) \leftarrow B^1\Pi_u(2, 83)$ and $2^1\Delta_g(1, 85) \leftarrow B^1\Pi_u(2, 84)$ transition, respectively. From Fig. 4, we obtain the intensity ratio of 0.01 for the $\Delta J = +1$ ($J = 82 \rightarrow J' = 83$) excitation transfer collision, which yields $R_{J \rightarrow J+1} = (0.01) / \tau_{J+1}$. Since

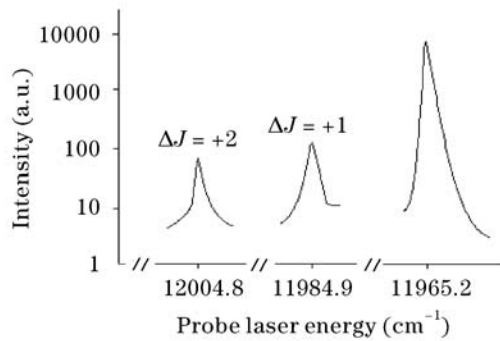


Fig. 4. Laser frequency scan showing the main line corresponding to $2^1\Delta_g(1, 83) \leftarrow B^1\Pi_u(2, 82)$ transition and the satellite peaks labeled $\Delta J = +1$ and $\Delta J = +2$.

τ_{J+1} is on the order of 8×10^{-9} s, we obtain an approximate value $R_{J \rightarrow J+1} = 1.25 \times 10^6 \text{ s}^{-1} \pm 45\%$. Similarly, we obtain $R_{J \rightarrow J+2} = 1.07 \times 10^6 \text{ s}^{-1} \pm 45\%$. The major sources of error in these rates are uncertainties in the intensity ratios and in $\tau_{J'}$.

This work was supported by the National Natural Science Foundation of China under Grant No. 10264004. Y. Shen is the author to whom the correspondence should be

addressed, his e-mail address is shenyifan01@sina.com. J. Liu's e-mail address is xdlj@sohu.com.

References

1. S. Antonova, G. Lazarov, K. Urbanski, and A. Marjatta Lyyra, *J. Chem. Phys.* **112**, 7080 (2000).
2. Y. Shen and K. Dai, *Chin. J. Lasers (in Chinese)* **31**, (Suppl.) 17 (2004).
3. L. Morgus, P. Burns, R. D. Miles, A. D. Wilkins, U. Ogba, A. P. Hickman, and J. Huennekens, *J. Chem. Phys.* **122**, 144313 (2005).
4. Z. J. Jabbour and J. Huennekens, *J. Chem. Phys.* **107**, 1094 (1997).
5. J. Huennekens, I. Prodan, A. Marks, L. Sibbach, E. Galle, and T. Morgus, *J. Chem. Phys.* **113**, 7384 (2000).
6. A. D. Wilkins, L. Morgus, J. Hernandez-Guzman, J. Huennekens, and A. P. Hickman, *J. Chem. Phys.* **123**, 124306 (2005).
7. Y.-F. Shen, A. Pulat, and K. Dai, *Chin. Phys. Lett.* **21**, 1934 (2004).
8. T.-J. Whang, H.-W. Wu, R.-Y. Chang, and C.-C. Tsai, *J. Chem. Phys.* **121**, 10513 (2004).
9. A. Corney, *Atomic and Laser Spectroscopy* (Clarendon Press, Oxford, 1977) p.244.